CHAPTER III

EXPERIMENTAL DETAILS

The present chapter is the description of the materials and methods employed in the synthesis and surface functionalization of polyaniline (PAni) nanofibers, polyaniline nanofibers:chitosan (PAni:Ch) nanocomposites and MEH-PPV:PCL nanofibers. The various physicochemical characterization tools such as TEM, SEM, XRD, Tensile test analyzer, TGA, I-V characteristics, contact angle measurement, XPS, FTIR spectroscopy, NMR spectroscopy, UV-Vis spectroscopy, fluorescence spectroscopy, have been explained herein. The assays for biological characterization of the synthesized conducting polymer (CP) based materials viz. Hemolysis assay, MTS cell proliferation assay, acridine orange/ethidium bromide (AO/EB) staining, live/dead assay and beta tubulin immunochemistry have been expounded in details. The experimental details for electrical stimulation of neuronal PC12 cells have been discussed as well.

3.1 Materials

Aniline (p.a. Merck Germany, ≥99.5%) was used for the synthesis of polyaniline (PAni) nanofibers. Aniline was distilled under reduced pressure before use. Ammonium peroxydisulfate (APS, p.a. Merck Germany, ≥98%) and hydrochloric acid (HCl, p.a. Sigma Aldrich, 37% AR grade) were used as oxidant and dopant, respectively, for synthesis of PAni nanofibers without further purification. Deionised water (12 MΩ cm) used for the synthesis was obtained from a Milli-Q system. Chitosan extrapure (p.a. SRL India, ≥99%) was used as received for synthesis of nanocomposite with PAni nanofibers. Acetic acid was purchased from (p.a. Sigma-Aldrich, ≥99.85%). 25% solution of Glutaraldehyde (p.a. Merck) was diluted to 1% using Milli-Q water for surface functionalization of PAni nanofibers and PAni nanofibers:Chitosan (PAni:Ch) nanocomposites. BOC glycine N-hydroxysuccinimide (NHS) ester (p.a. Acros Organics, ≥99%) and trifluoroacetic acid (TFA, p.a Sigma-Aldrich, 99%) were used for surface functionalization of PAni:Ch nanocomposites.

Table 3.1: Some physical properties of materials used in the synthesis and surface functionalization of PAni nanofibers and PAni:Ch nanocomposites.

Physical properties of the monomer						
Monomer	**Molecular structure**	**Molecular weight** g/mol	**Melting point (^{0}C)**	**Boiling point (^{0}C)**	**Density at 25^0 C (g/mL)**	**Oxidation potential (Volt)**
Aniline	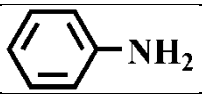	93.13	-6	184	1.022	0.9
Physical properties of the biopolymer						
Biopolymer	**Molecular structure**	**Molecular weight g/mol**	**Viscosity (20°C) m.Pas**	**Deacetylated Degree**		
Chitosan	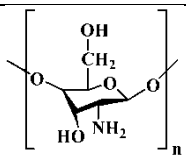	1526.464	150-500	90%		
Physical properties of the functionalizing agents						
Reagent	**Molecular structure**	**Molecular weight g/mol**	**Melting point (^{0}C)**	**Boiling point (^{0}C)**	**Density g/mL**	
Glutaraldehyde	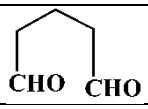	100.117	-14	187	1.06	
BOC-Glycine N-hydroxysuccinimide ester	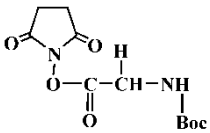	272.26	158.4-161.9	-	-	
Physical properties of the oxidant and dopant						
Reagent	**Molecular structure**	**Molecular weight g/mol**	**Melting point (^{0}C)**	**Boiling point (^{0}C)**	**Density g/mL**	
Ammonium persulfate	$[NH_4]_2S_2O_8$	228.20	120	-	1.98	
Hydrochloric acid	HCl	36.48	-	>100	1.20	
Physical properties of the solvents						
Solvent	**Molecular formula**	**Molecular weight g/mol**	**Melting point (^{0}C)**	**Boiling point (^{0}C)**	**Density g/mL**	
N-Methyl-2-pyrrolidone	C_5H_9NO	99.13	-24	204	1.028	
Acetic acid	CH_3COOH	60.05	16	118	1.049	
1-Ethyl-3-(3-dimethylaminopropyl)carbodiimide	$C_8H_{17}N_3$	155.25	111-113	-	-	
Trifluoroacetic acid	$C_2HF_3O_2$	114.02	-15.4	72.4	1.489	

Table 3.2: Some physical properties of MEH-PPV used in electrospinning of MEH-PPV:PCL nanofibers.

Physical properties of the CP					
Polymer	**Molecular structure**	**Molecular weight** g/mol	**Melting point (^{0}C)**	**Boiling point (^{0}C)**	**Thermal degradation (°C)**
MEH-PPV	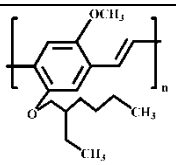	150,000-250,000	190	-	371

Physical properties of the biopolymer					
Biopolymer	**Molecular structure**	**Molecular weight g/mol**	**Melting point (^{0}C)**	**Boiling point (^{0}C)**	**Density g/mL**
PCL	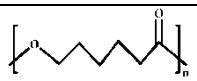	80,000	60	-	1.145

Physical properties of the functionalizing agents					
Reagent	**Molecular structure**	**Molecular weight g/mol**	**Melting point (^{0}C)**	**Boiling point (^{0}C)**	**Density g/mL**
(3Aminopropyl) triethoxysilane	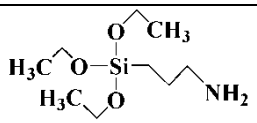	221.37	-70	217	0.946
1,6-Hexanediamine	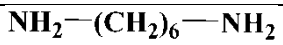	116.21	39	204.6	0.84

Physical properties of the dopant and solvents					
Reagent	**Molecular formula**	**Molecular weight g/mol**	**Melting point (^{0}C)**	**Boiling point (^{0}C)**	**Density g/mL**
Ferric chloride	$FeCl_3$	162.2	306	315	2.898
Dichloromethane	CH_2Cl_2	84.93	-96.7	39.6	1.3266
Dimethylformamide	C_3H_7NO	73.10	-60.5	154	0.948
Chloroform	$CHCl_3$	119.37	-63.5	61.15	1.489
Ethanol	C_2H_6O	46.07	-114.14	78.24	0.7893
Isopropanol	C_3H_8O	60.10	-89	82.6	0.786

Poly[2-methoxy-5-(2-ethylhexyloxy)-1,4-phenylenevinylene] (MEH-PPV, Sigma-Aldrich, UK), Polycaprolactone (PCL, Sigma-Aldrich, UK), Chloroform (≥99.5%, Sigma-Aldrich, UK), Dimethylformamide (≥99.8%, Sigma-Aldrich, UK), Dichloromethane (≥99.8%, Sigma-Aldrich, UK), Iron(III) chloride ($FeCl_3$, anhydrous, powder, ≥99.99%, Sigma-Aldrich, UK) were used for electrospinning without further

purification. (3-Aminopropyl)triethoxysilane (APTES, ≥99%, Sigma-Aldrich, UK) and 1,6-Hexanediamine (≥99%, Sigma-Aldrich, UK) were used as obtained.

All other chemicals, solvents and reagents used in the synthesis and purification process were of analytical grade and used as received without any further purification. The physical properties of the materials used for the synthesis of different PAni based nanostructured materials and MEH-PPV based materials in the present work are tabulated in **Table 3.1** and **Table 3.2,** respectively.

3.2 Synthesis and surface functionalization of conducting polymer (CP) based nanostructures

3.2.1 Synthesis of polyaniline (PAni) nanofibers

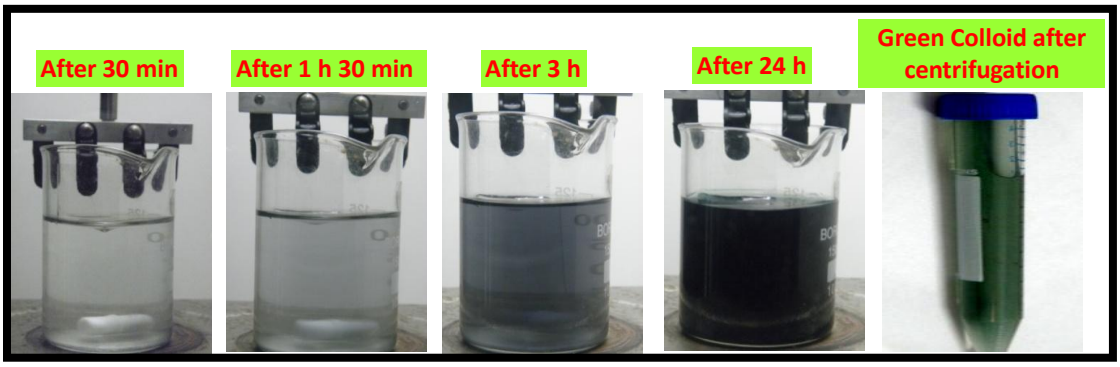

Figure 3.1. Images illustrating dilute polymerization of polyaniline (PAni) nanofibers.

Polyaniline (PAni) nanofibers were synthesized using the method described by Chiou *et al*. [210, 267]. A solution of 1M HCl (dopant acid) was prepared and the monomer aniline was dissolved in a small portion of that solution. Ammonium peroxydisulfate (APS) was dissolved in the remaining portion of the dopant acid solution. The monomer solution was then carefully transferred to the solution of APS. The reaction was allowed to take place in a magnetic stirrer at a very slow stirring rate at room temperature for about 24 h till the whole mixture became dark green [**Figure 3.1**]. The whole mixture was then filtered and washed with deionised water until the filtrate became colourless. The initial concentration of aniline in the reaction mixture was kept at 8 mM and the molar ratio of the monomer to the oxidant was maintained at

2:1. PAni films were prepared as reported earlier [300]. First, the as-synthesized PAni nanofibers were washed with 25-30% ammonia solution for 3 times to make it emeraldine base. Then, 500 mg of finely ground PAni nanofibers (PNFs) has been magnetically stirred in 30 mL of NMP solution for 8 h after which the intense blue solution was again sonicated so that the PNFs become completely dissolved. A pasteur pipette was used to cast the films on clean glass slides from this solution. The casted glass then dried in an oven at 60°-70°C for 4 h and after drying, films can be removed by immersing the glass slides in water for 5-10 min.

3.2.2 Surface functionalization of polyaniline (PAni) nanofibers

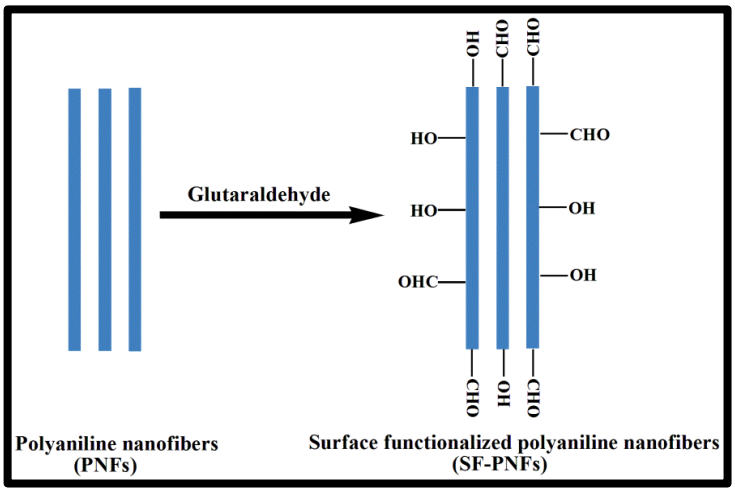

Figure 3.2. Schematic representation of surface functionalization of polyaniline (PAni) nanofibers by glutaraldehyde.

Surface Functionalization of the PNFs was accomplished by treating the purified PNFs with 1% glutaraldehyde in phosphate buffer saline (PBS, pH=7.4) for a period of 24 h to introduce polar hydroxyl (-OH) and aldehyde (-CHO) on the surface **[Figure 3.2]**. There are two reasons of using 1% glutaraldehyde for surface functionalization of PAni films. Firstly, glutaraldehyde generally is considered to be toxic. So, the higher amount of glutaraldehyde may be harmful for the cells and thereby, restricts its biological applications. This particular amount of glutaraldehyde (1%) was found to be cytoampatible with peripheral blood mononuclear cells (PBMCs) as shown in **Figure 3.3**. 1% glutaraldehyde in a 2 mL volume is equivalent

to 8 μL from a 25% glutaraldehyde stock solution (Merck). In **Figure 3.3**, 4 μL/mL is equivalent to 1% glutaraldehyde, which demonstrates maximum cell viability.

Secondly, the higher amount glutaraldehyde reduces the stability of the PAni films as we had observed during surface functionalization of PAni films with different amounts of glutaraldehyde.

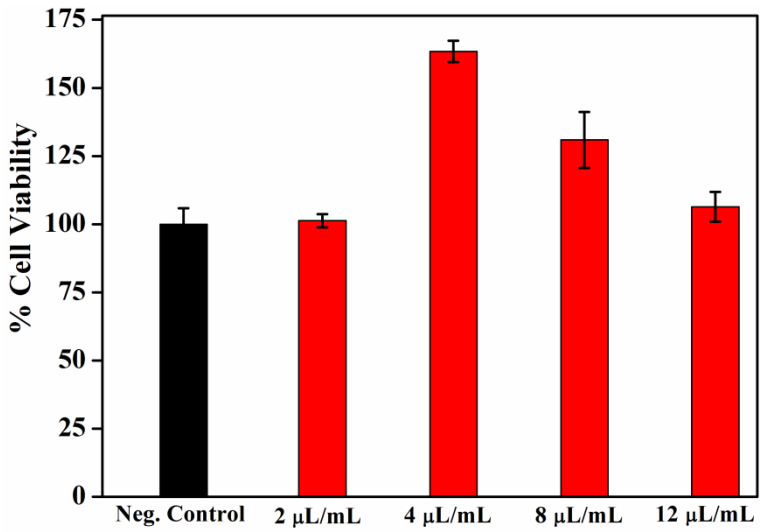

Figure 3.3. Percentage of cell viability of PBMC for 1% glutaraldehyde solution at three different doses. As the concentration of the doses increases, percentage of cell viability observed to be decreased. It indicates the biocompatibility nature of glutaraldehyde at lower dose level.

Subsequently, the surface functionalized PAni nanofibers (SF-PNFs) were washed with deionised water to remove the excess glutaraldehyde. The reason for choosing glutaraldehyde as a surface functionalization agent was its high reactivity towards the amine group [301] and as such it has been often used as a cross-linking agent. The molecular form of glutaraldehyde in aqueous solution enables it to cross-link two materials having active amine groups [301]. Thus, it was expected that the SF-PNFs would be highly reactive towards other chemical species having active amine groups such as amino acids and enzymes. Also, it has been reported earlier that glutaraldehyde is the most effective cross-linking agent [25] due to its easy commercial availability and low cost in addition to high reactivity.

3.2.3 Synthesis of polyaniline nanofibers:chitosan (PAni:Ch) nanocomposites

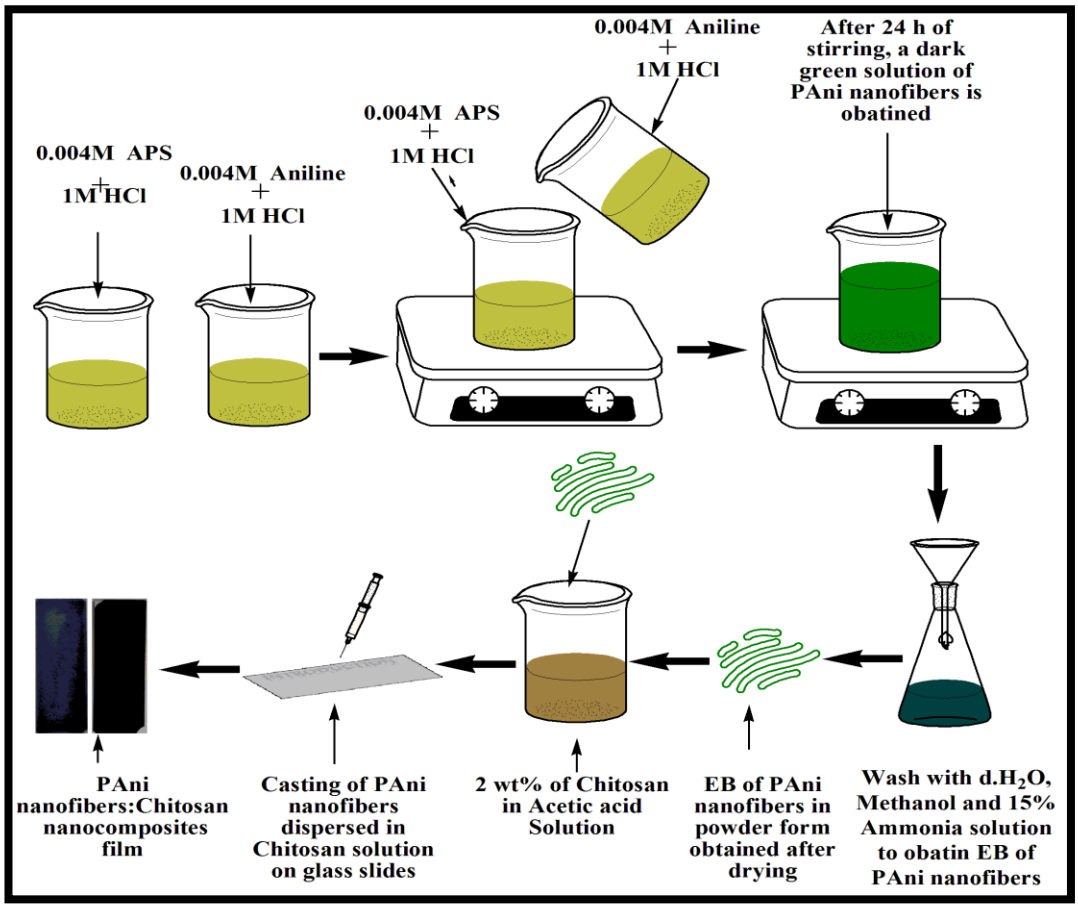

Figure 3.4. Schematic representation of synthesis of and polyaniline (PAni) nanofibers and polyaniline nanofibers:chitosan (PAni:Ch) nanocomposites.

Polyaniline nanofibers:chitosan (PAni:Ch) nanocomposites were prepared with slight modification as shown in Figure 3.4 [302]. Chitosan (Ch) solution was prepared in 2 % (v/v) acetic acid solution. PNFs were added to the chitosan solution at concentrations of 4 % and 6 % (w/v) and the mixture was ultra-sonicated the mixture for one hour. The resultant solution was then casted onto a glass slide using a pasteur pipette and dried at 60°-70°C for 4 hours. The films were then removed by immersing the glass slides in water for 5-10 minutes.

3.2.4 Surface functionalization of polyaniline nanofibers:chitosan (PAni:Ch) nanocomposites

3.2.4.1 Using glutaraldehyde

Surface Functionalization of the PAni:Ch nanocomposites was accomplished by treating the as-prepared PAni:Ch nanocomposites films with 1% glutaraldehyde in phosphate buffer saline (PBS, pH=7.4) for 15 min. After 15 min, the films were washed thrice with distilled water to remove the unbound glutaraldehyde and air-dried before use.

3.2.4.2 Using BOC-Glycine N-hydroxysuccinimide (NHS) ester

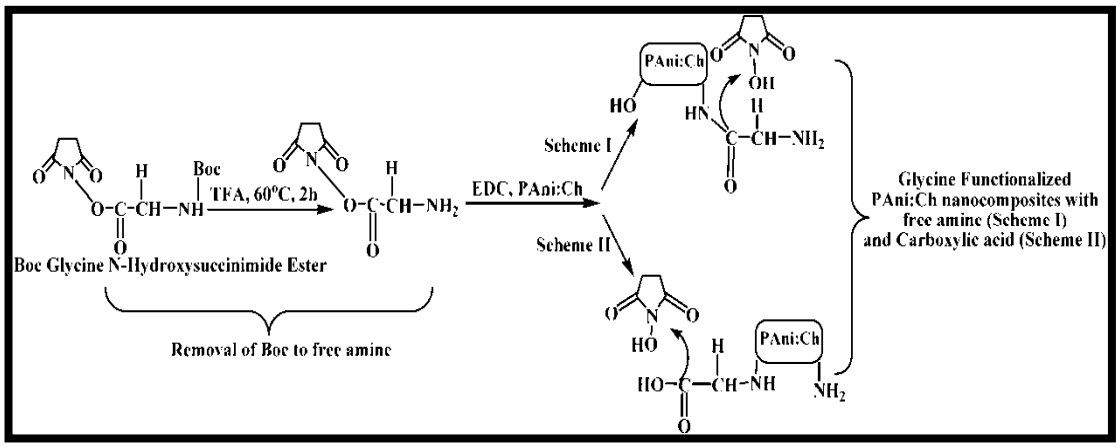

Figure 3.5. Schematic representation of the surface functionalization of polyaniline nanofibers:chitosan (PAni:Ch) nanocomposites using BOC glycine-NHS ester.

BOC glycine N-hydroxysuccinimide (NHS) ester was treated with trifluoroacetic acid (TFA) for 2h at 60^{o}C to remove the amine protecting BOC (*tert*-butyloxycarbonyl) part. Following BOC removal, unprotected glycine NHS ester was obtained after filtration and washing with deionised water to make sure that there are no TFA molecules left out. This washing step is expected to diminish the probability of any byproducts formed due to side reactions e.g. TFA with NHS ester. Then, the BOC removed glycine NHS ester was air dried for 1 h. Glycine NHS ester is insoluble in water and it is believed that treatment with water doesn't effect it. After that, a solution of 10 mmol of 1-eEthyl-3-(3-dimethylaminopropyl) carbodiimide (EDC) was

made in distilled water. 5 mmol of glycine NHS ester is added to the above solution and dissolved under 30 min of stirring. This was performed according to the previous report [303]. EDC has been used in the coupling protocols to improve efficiency or create dry-stable (amine-reactive) intermediates. One of the main advantages of EDC coupling is its water solubility, which allows direct bioconjugation without prior organic solvent dissolution. PAni:Ch nanocomposite films cut into circular shapes of 5 and 10 mm in diameter were immersed into the above mixture for 20-30 min. at room temperature. The treated nanocomposites films were washed with dimethyl sulfoxide (DMSO) thrice and air dried. Due to good solubility in DMSO, any unbound glycine-NHS ester or glycine oligomers formed, can be easily removed through the washing step. That ensures the final surface functionalized PAni:Ch films free from any glycine oligomers or any other probable side reactions related byproducts. Thereby, all the side reaction products will have no role in further experimentation. The schemes of surface functionalization of PAni:Ch nanocomposites using BOC glycine-NHS ester are shown in **Figure 3.5**.

3.2.5 Electrospinning of MEH-PPV:PCL nanofibers

3.2.5.1 Doping of MEH-PPV

MEH-PPV was doped using $FeCl_3$ as a p-type dopant as reported by Shin Sakiyama *et al* [83]. Briefly, $FeCl_3$ was dissolved in dehydrate ethanol at a concentration of 3 mg/mL and kept stirring overnight at 50°C overnight in a laminar hood. 0.5 wt% MEH-PPV was dissolved in a solution mixture of chloroform and dimethylformamide (DMF) of 60:40 (v/v). The dopant solution was added to MEH-PPV solution at a concentration of 2 wt% against the polymer and stirred for 30 min. The resultant solution of MEH-PPV containing dopant $FeCl_3$ was used in electrospinning.

3.2.5.2 Simple electrospinning of MEH-PPV:PCL nanofibers

PCL was dissolved in a solution of dichloromethane (DCM) and dimethylformamide (60:40 v/v) at a concentration of 14 wt%. $FeCl_3$ doped MEH-PPV solution was mixed with PCL solution at four volume ratios of 20:80 (v/v), 40:60 (v/v), 50:50 (v/v) and 60:40 (v/v). MEH-PPV and PCL solutions were stirred for 1-2 h at 100-150°C to obtain a complete dispersed solution for electrospinning. For electrospinning, the mixed polymer solution was fed into a 10 mL standard plastic syringe equipped with a

30-gauge stainless steel needle and electrospun using a syringe pump (KDS 200, KD Scientific Inc., USA) at a potential of 18 kV from a high voltage power supply (Spellman, UK) and flow rate of 0.5 mL/h. The schematic of the electrospinning process is shown in **Figure 3.6 (a)**. Electrospun fibers were collected on an aluminium foil wrapped copper plate at a distance of 16 cm from the syringe needle tip. The as-spun nanofibrous meshes were air dried for overnight to remove the residual solvent and carefully removed from the aluminium foil for further investigation. All experiments were conducted at room temperature of 18-22°C with an average humidity of 60-65%.

3.2.5.3 Coaxial electrospinning of MEH-PPV:PCL nanofibers

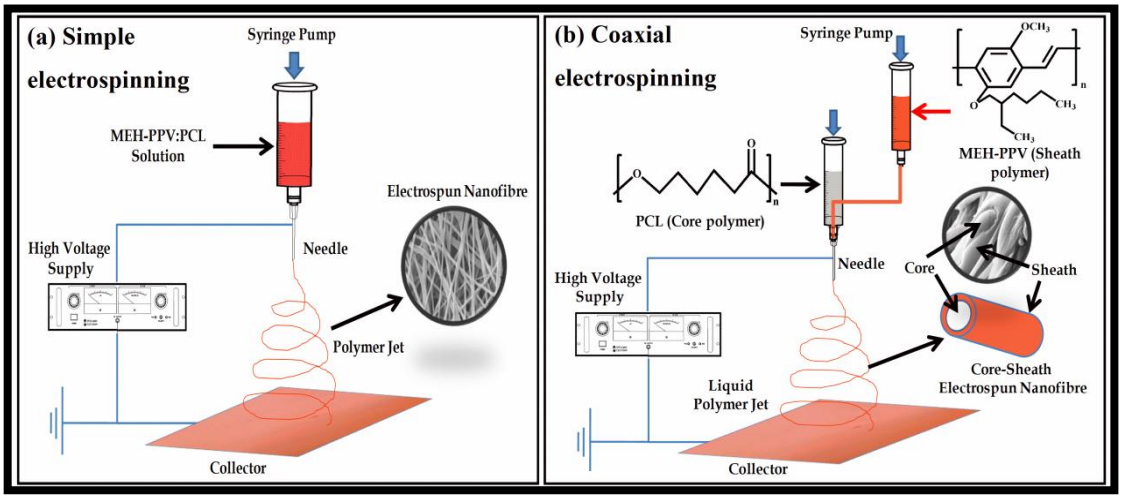

Figure 3.6. Schematic representations showing electrospinning of MEH-PPV:PCL by (a) simple electrospinning process and (b) coaxial electrospinning process.

For coaxial electrospinning, both PCL solution and MEH-PPV solution, prepared as described above, were fed into two 5 mL standard plastic syringe separately attached to a coaxial spinneret. The schematic of coaxial electrospinning was shown in **Figure 3.6 (b)**. The flow rate was adjusted in a two-way syringe pump. The coaxial spinneret was connected to the same electrical potential, provided by a high voltage power supply. The coaxial electrospinning was carried out at two flow rates of 0.6 mL/h and 1 mL/h at an applied voltage of 20 kV and a 15 cm needle tip to collector (copper plate wrapped with aluminium foil) distance. After electrospinning, the deposited meshes were air dried for overnight and carefully removed from the aluminium foil.

All experiments were conducted at room temperature of 18-22°C with an average humidity of 60-65%. Photograph acquired during coaxial electrospinning of MEH-PPV:PCL nanofibers is shown in **Figure 3.7**.

Figure 3.7. Photograph of coaxial electrospinning of MEH-PPV:PCL nanofibers.

3.2.5.4 Surface functionalization of MEH-PPV:PCL nanofibers

3.2.5.4.1 Using (3-Aminopropyl)triethoxysilane (APTES)

Electrospun meshes were surface functionalized by APTES to improve the surface hydrophilicity as reported earlier [304]. Briefly, electrospun meshes are treated in 10 % (v/v) solution of APTES in ethanol for 18 h at room temperature. After treatment with APTES, electrospun meshes were washed with ethanol and distilled water twice to remove any unbound APTES molecules and air dried for 3 h.

3.2.5.4.2 Using 1,6-Hexanediamine

The surface of the electrospun meshes was functionalized using 1,6-Hexanediamine as reported elsewhere [305]. Typically, electrospun meshes are treated in 5 wt% solution of 1,6-Hexanediamine in isopropanol for 3 h at 40°C. After treatment with

1,6-Hexanediamine, electrospun meshes were washed with isopropanol and distilled water thrice to remove any unbound molecules and air dried for 3 h.

3.3 Characterization techniques

3.3.1 Transmission electron microscopy (TEM)

Transmission electron microscopy (TEM) is a versatile technique to study the microstructure of materials at the nanometer level, with resolutions in the order of a few tenths of a nanometer. TEM can also provide informations on diffraction pattern of a material from specific regions in the images as small as 1 nm [306]. In TEM, a high voltage electron beam emitted by an electron gun is being focussed with the help of electromagnetic lenses to produce an image of internal microstructure of a sample. The high voltage electron beam accelerated by an anode typically in the range 40 to 400 keV with respect to the cathode passes through the sample in part and carries the information of the internal microstructure of the sample upon emerging [307]. The spatial information is magnified by the objective lens system of the microscope followed by projection of the magnified electron image onto a phosphor or a scintillator material such as zinc sulfide coated fluorescent screen. The image can be photographed by exposing a photographic plate directly to the electron beam or by coupling of a high-resolution phosphor with a lens system or a fiber optic light-guide to a charge-coupled device (CCD) camera followed by being displayed in computer monitor. Although the resolution of the TEM image is limited spherical aberration, appropiate spherical aberration correction can enable the production of the image at a resolution below 0.5 Å at a magnification above 50000K [307].

The TEM studies have been carried out using TECNAI G2 20 S-TWIN (200KV); Resolution: 2.4A0, transmission electron microscope (FEI COMPANY, USA) installed at Sophisticated Analytical Instrumentation Centre (SAIC) at Tezpur University, India. The micrographs have been taken at 100 kV accelerating voltage at different magnifications according to need. For TEM, the as-synthesized PAni nanofibers were dispersed in ethanol, whereas the core-sheath MEH-PPV:PCL nanofibers were dispersed in tetrahydrofuran (THF). The sonication step during sample preparation of MEH-PPV:PCL in THF was skipped. It has been observed that sonication of the same breaks the fibers easily and it get dissolved rather being get dispersed uniformly, what is required for TEM measurement. The samples were

prepared on carbon coated copper grids for viewing under TEM. TEM image of each sample was acquired at four different regions and for evaluation of the diameter distribution, four images have been analyzed using ImageJ software.

3.3.2 Scanning electron microscopy (SEM)

Scanning electron microscopy (SEM) is a premier tool for microstructural analysis of materials. The SEM provides information relating to topographical features, morphology, phase distribution, compositional differences, crystal structure, crystal orientation, and the presence and location of electrical defects [308]. During SEM characterization, a moderately high energetic electron beam is focused onto the sample specimen with the help of electromagnetic fields, while the SEM optical column ensures that the incoming electrons are of same energy and trajectory. The electron beam interacts with the atoms of the specimen in elastically and inelastically. Elastic interactions cause a change in trajectory of the electron beam without energy loss, while inelastic interactions aid energy transfer to the atoms of the sample specimen. Due to the multiple interactions of the electrons, the electron beam spreads out into the material through simultaneous energy loss and change in trajectory and produces an interaction volume within the material. Each signals corresponding to different interaction have different depths within the specimen from which they can escape due to their unique physical properties and energies.

Lenses used in the SEM demagnify and focus the electron beam onto the sample surface, giving rise to two major benefits of the SEM, viz., range of magnification and depth of field in the image. This permits surfaces at various distances from the lens to appear to be focused for three dimensional image productions [308]. As discussed above, the interaction of highly energetic electrons with the atoms on the sample surface generate backscattered electrons (BSEs) and secondary electrons (SEs). BSEs with higher average energy than that of SEs, emanating from the incident probe suffer elastic interactions, trajectory change, and escape from the sample surface. BSEs, which depend upon the average atomic number (Z) of the specimen, make up the most of the emitted electrons from the specimen at a high voltage. Therefore, heavier elements produce more BSEs. The BSE intensity and trajectory also depend upon the angle of incidence between the beam and the specimen surface.

Then, the BSE signal is used to generate the surface topography of the sample specimen. SEs, emitted from an outer shell of a specimen atom with energy typically in the range 2 to 5 eV, are produced due to inelastic interactions and dictated by surface properties. Since SEs are of relatively lower energy than that of BSEs, SEs escape is generally between 5-50 nm. The generation of SEs occur due to the beam entering the specimen and BSEs as they escape the specimen, however, the generation is around the initial probe diameter. The intensity of SEs is a function of the surface orientation with respect to the beam and the SE detector and hence can record the specimen morphology [308].

The SEM study for the PAni based materials were acquired using a JEOL JSM 6390 LV model scanning electron microscopy installed at Central Instrumentation Facility (CIF), Tezpur University, Assam, India to examine the surface morphology and porosity. The micrographs have been taken at an accelerating voltage varying between 5-15 kV and magnification is fixed according to need from 2000X to 10000X. The samples have been coated with platinum and placed on carbon tape before viewing.

The SEM of various MEH-PPV based electrospun meshes were recorded using Carl Zeiss SIGMA FEG-SEM installed at University of Brighton, UK. FEG-SEM equipped with the GEMINI column with its in-lens secondary electron detection, provides unparalleled resolution, contrast and brightness for imaging highly topographical samples. The GEMINI column design provides superb low voltage imaging and stability allowing excellent imaging for beam sensitive and non-conducting specimens. The electron source is a field emission gun, which emits electrons in a parallel beam enabling better spatial separation of objects of interest so that structures as small as (circa) 1.5 nm can be resolved.

3.3.3 X-ray diffraction (XRD)

X-ray scattering and spectroscopy methods can provide valuable information regarding the physical and electronic structure of crystalline and non-crystalline materials in a variety of external conditions and environments. X-ray powder diffraction is one of the most widely used probes for crystal structure determination. This technique is based on the scattering of X-rays by crystals governed by the Bragg's law. Powder X-ray diffraction is used to determine the atomic structure of

crystalline, semi-crystalline and amorphous materials without the need for large (~100 μm) single crystals. X-ray diffraction patterns give information about crystal structure parameters like crystallite size (domain length in case of semi-crystalline polymers), *d*-spacing, diffraction planes, structure, phase and lattice constants. In addition to the crystal structure, XRD is applied for various other purposes such as chemical analysis, stress, strain, particle size measurements, phase equilibrium, determination of orientation for single crystals or the ensemble of orientations in a polycrystalline or polymeric aggregate, order-disorder transformation etc. The intensities and angles of the diffracted X-ray beams are related to the atomic arrangement of the crystal.

In case of polymeric materials, XRD is used to determine the proportions of the crystalline and amorphous phases in terms of the degree of crystallinity. X-ray diffraction is also used to determine the domain length in case of polymers. Polymers are semi-crystalline materials. Their crystallinity is attributed to chain folding or to the formation of single or double helices, for at least part of their chain length [309]. This local range of order in polymer chains is referred to as the domain length (*L*) and can be in the range of angstroms (Å). The X-ray diffraction patterns for the polyaniline (PAni) based nanostructured materials and MEH-PPV based electrospun materials reported in the present work were recorded using a D8 FOCUS, Bruker Axs, Germany diffractometer with Cu K_α radiation (λ = 1.5406 Å). The angular range spread over the region between 10^0 and 70^0 in 2θ, in steps of 0.05^0. The X-ray diffraction patterns have been used to determine the *d*-spacings, domain length (*L*), strain (ε), and the degree of crystallinity. The methodology adopted for the quantitative estimation of these structural details of the PAni based nanostructured materials specifically the *d*-spacings, domain length (*L*), strain (ε) and the degree of crystallinity are discussed in the following subsections.

3.3.3.1 Calculation of d-spacing, domain length (L) and strain (ε)

The *d*-spacings have been determined from the angular position (2θ) of the observed peaks in the X-ray diffraction patterns of the PAni based nanostructured materials, according to the Bragg's formula as follows

$$\lambda = 2d \sin\theta \qquad 3.1$$

Line broadening in the x-ray diffraction patterns is due the size and strain

components. The former depends on the size of coherent domains (or incoherently diffracting domains), which is not limited to the grains but may include effects of stacking and twin faults and sub-grain structures (small-angle boundaries, for instance); and the latter is caused by any lattice imperfection (dislocations and different point defects) [310]. This theory has been successfully applied to all forms of materials, including oxides and polymers [311].

In the present work, the domain length (L) and strain (ε) of the PAni nanofibers and MEH-PPV based electrospun nanofibers have been calculated using a single line approximation technique employing Voigt function [312]. The measures of dispersion used in earlier studies of crystal imperfections by means of diffraction broadening have been the width of the line profile at half the maximum intensity (FWHM, $2w$) and the integral breadth (β). However, uncertainties arising from the correction of the instrumental broadened in the profile have led to the introduction of the Fourier and variance methods [313]. These methods allow a detailed and accurate analysis of imperfections to be undertaken, but are solely dependent on the quality of the data, necessary expertise and computing facilities that are available to analyse the data.

A limitation in the use of the FWHM or integral breadth is the need to ascribe an analytical function to the line profiles. Earlier workers have assumed that they are Cauchy (Lorentzian) or Gaussian in form, but it has been demonstrated later on [314] that a closer approximation is given by the convolution of these curves, namely the Voigt function. The Voigt function has been adopted by many groups for an analysis of diffraction broadening based on the integral breadth of a single line and the approach has also been used to obtain the domain size and strain in deformed tungsten [312]. An explicit equation for the Voigt function has been introduced by Langford in 1978 [315], which shows that the breadths of the Cauchy and Gaussian components can easily be found from the ratio of the FWHM of the broadened profile to its integral breadth ($2w/\beta$). Later on Keijser *et al.* [312] reported that graphical methods or interpolation from tables can be avoided by using empirical formulae and thus the required calculations can be simplified greatly. While it is always desirable to use data from several reflections whenever practicable, the method can be used in single-line analysis.

The measured line profile *h* is the convolution of the standard profile *g* with the structurally broadened profile *f*. Assuming, *h*, *f* and *g* to be Voigt functions [315], we get,

$$h_C = g_C \otimes f_C \; and \; h_G = g_G \otimes f_G \qquad 3.2$$

where subscripts C and G denote the Cauchy and Gaussian components of the respective Voigt profiles. From *Equation 3.2*, it follows that the integral breadths of f_C and f_G, are given by

$$\beta_C^f = \beta_C^h - \beta_C^g \; and \; \left(\beta_G^f\right)^2 = \left(\beta_G^h\right)^2 - \left(\beta_G^g\right)^2 \qquad 3.3$$

The constituent Cauchy and Gaussian components can be obtained from the ratio $2w/\beta$ for the *h* and *g* profiles. However, to avoid graphical methods or interpolation from tables, an empirical formula has been given as [312]:

$$\beta_C = (a_o + a_1\varphi + a_2\varphi^2)\beta \qquad 3.4$$

and

$$\beta_G = \left[b_o + b_{12}\left(\varphi - \frac{2}{\pi}\right)^{1/2} + b_1\varphi + b_2\varphi^2\right]\beta \qquad 3.5$$

where $\varphi = 2w/\beta$, $a_0 = 2.0207$, $a_1 = -0.4803$, $a_2 = -1.7756$, $b_0 = 0.6420$, $b_{12} = 1.4187$, $b_1 = -2.2043$ and $b_2 = 1.8706$.

The maximum error introduced by *Equation 3.4* and *Equation 3.5* is about 1%, and in the majority of cases the error is much less than this. In order to separate size and strain effects, it has been assumed that the size and strain profiles have a Voigtian profile. If two or more reflections are available, size and strain effects can be determined from the variation of β_C^f and β_G^f with *hkl* [315]. However, in a single-line analysis it is assumed that the Cauchy component of the *f* profile is solely due to crystallite size (domain length in case of polymers) and that the Gaussian contribution arises from strain [316]. In a single-line analysis the apparent crystallite or domain length (*L*) is given by [312]:

$$L = \frac{\lambda}{\beta_C^f \cos\theta} \qquad 3.6$$

and the strain (ε) is given as

$$\varepsilon = \frac{\beta_G^f}{4\tan\theta} \qquad 3.7$$

where β is measured on a 2θ scale and, if K_α radiation is used, λ and θ are the wavelength and angular position of the α_1 component.

3.3.3.2 Degree of crystallinity

Domain length (L) is a measure of the local range of order (ordering in a single polymer chain) of a polymer whereas the overall ordering in the polymer samples are generally described in terms of the degree of crystallinity. The degree of crystallinity gives quite a good estimation of the amount of crystalline phase present in a polymer sample. A typical X-ray diffractogram for a polymeric material consist of a broad amorphous hump superimposed with some sharp peaks as shown in the **Figure 3.8 (a).** The total area under the diffractogram is the sum of the crystalline peaks and broad amorphous hump.

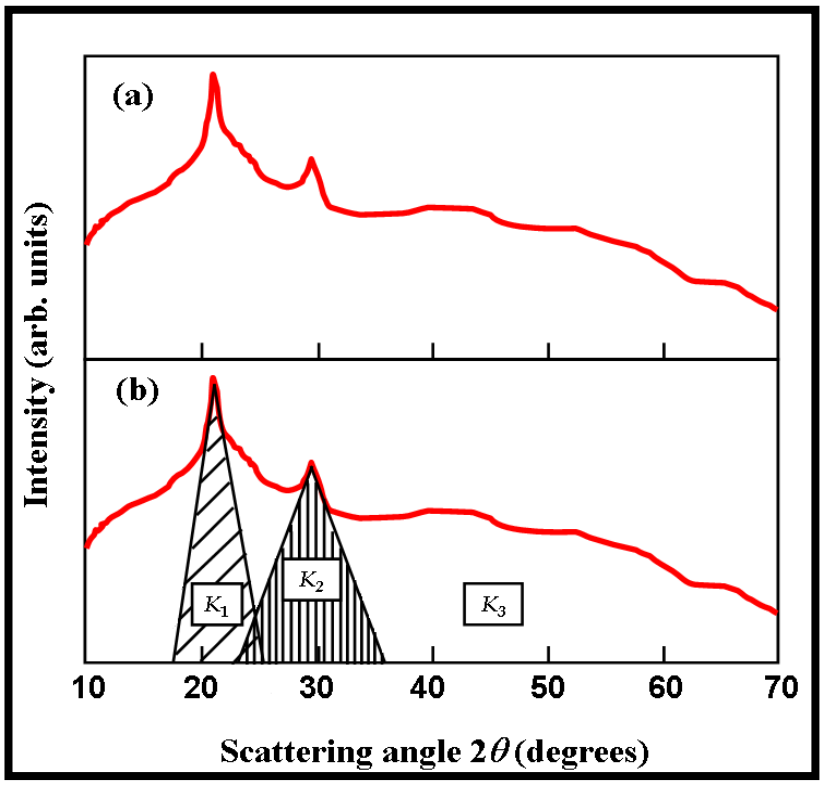

Figure 3.8. (a) Typical X-ray diffractogram of a semi-crystalline polymer and (b) XRD patterns showing the superposition of crystalline peaks and an amorphous hump.

If a typical X-ray diffractogram has two crystalline peaks with areas K_1 and K_2 superimposed on a broad amorphous hump with an area K_3 as shown in **Figure 3.8 (b)**, then the degree of crystallinity (κ) of the polymer will be

$$\kappa = \frac{\alpha_C(K_1 + K_2)}{\alpha_C(K_1 + K_2) + \alpha_A K_3} \quad 3.8$$

where α_C and α_A are proportionality constants for the crystalline and amorphous phases, respectively. Assuming $\alpha_C = \alpha_A$ for reasonable accuracy in polymers, the *Equation 3.8* for the degree of crystallinity may be written as

$$\kappa = \frac{K_1 + K_2}{K_1 + K_2 + K_3} = \frac{K}{K_o} \quad 3.9$$

In order to express the degree of crystallinity in the form of percentage, the above *Equation 3.9* can be modified as:

$$\kappa = \frac{K_1 + K_2}{K_1 + K_2 + K_3} \times 100\% = \frac{K}{K_o} \times 100\% \quad 3.10$$

where *K* is the sum of the areas of all the crystalline peaks in the diffractogram and K_0 is the total area under the diffractogram. In the present work the area has been calculated by dividing the X-ray diffractogram into minute square grids (0.5x0.5 mm^2) and counting the number of grids. The degree of crystallinity of a polymer is affected by the secondary valence bonds that can be formed, the structure of the polymer chain (range of order), the physical treatment and the molecular weight of the polymer.

3.3.4 Thermogravimetric analysis (TGA)

Thermogravimetric analysis (TGA) is a technique in which the weight loss of a material is monitored as a function of temperature at a constant heating rate or isothermally as a function of time, as the sample specimen is subjected to a controlled temperature programme in a controlled atmosphere. TGA consists of a sample pan, which is supported by a precision balance. The pan is placed in a furnace and heated or cooled during the experiment. The atmosphere in the sample chamber is purged with an inert gas to prevent oxidation or other undesired reactions. As the temperature increases, the various components of the samples are decomposed and the weight percentage of each resulting mass change is monitored as a function of temperature. Results are presented with temperature along X-axis and mass loss along Y-axis. Its principal uses include measurement of a material's thermal stability and composition. The TGA analysis of all the materials discussed in the current study were performed

using a Perkin Elmer, model STA 6000 thermogravimetric analyzer installed at Materials Research Laboratory, Department of Physics, Tezpur University.

3.3.5 Current-voltage (I-V) characteristics

In order to fulfil the potential applications of conducting polymer nanostructures, it is necessary to understand the electronic transport properties of the nanostructures. Determination of conductivity of these nanostructures is critical for application point of view. Two probe *I-V* measurements are considered as the simplest approach in order to understand the conductivity of a material. A current-voltage characteristic is a relationship typically representing a graph of electric current with respect to the applied voltage. Steady state current voltage measurement of the samples were performed by two probe technique using Keithley 2450 source meter. *I-V* measurements were performed by applying a DC voltage sweep from 0 to ±10 V, and measuring the resulting current. All the *I-V* measurements were carried out in film form at room temperature (~300K).

The sheet resistance (R_s) values of all the materials synthesized during the current study were determined using the formula given below [139, 155]:

$$Sheet\ resistance\ (R_s) = R \times \frac{W}{D} \qquad 3.11$$

Where W is the sample width and D is the distance between the two probes of the source meter. R is determined from the inverse of the slope of the *I-V* characteristics.

3.3.6 Mechanical property measurement

The mechanical properties of the as-synthesized materials before and after surface functionalization were evaluated using a TA.XT *plus*Texture Analyser (Stable Micro System) equipped with a 2 kg load cell, installed at University of Brighton, UK. Film strips with dimensions of 10 mm by 50 mm and free from air bubbles or physical imperfections, were held between the two clamps positioned at a distance 2 cm. During, measurement, the film was pulled by the top clamp at a rate 0.5 mm/s to a distance of 5 cm before returning to the starting point. The force and elongation were measured when the films broke. Measurements were repeated three times for each film. The Young's modulus or stiffness constant (*E*) was determined directly from the slope of the stress *vs.* strain curve.

3.3.7 Contact angle measurements

Static contact angle measurements were carried out by the sessile drop method to evaluate the effect of surface functionalization on wettability and the surface free energy. Contact angle measurement is first described in qualitative form by Thomas Young in 1805, which is used for determination of the interaction between a liquid and solid at the minimum equilibrium distance [317].

The value of contact angle (θ) is a measure of the competing addiction between the cohesive energy among the liquid molecules and the between the liquid and the solid surface. When the cohesive energy exceeds the adhesive energy, a liquid drop on a solid surface conceives a finite contact angle. In contrast, when the adhesive energy is more than the cohesive energy, the liquid drop spreads out on the surface. Wettability is strongly correlated to the surface adhesion property. Measurement of wettability is the most commonly performed and the simplest surface sensitive analysis technique. In addition, the determination of solid-vapour and solid-liquid interfacial tension is of importance in a wide range of problems in pure and applied science. The measurement of contact angle on a given surface is considered as the most practical way for the estimation of surface energy [297].

Contact angle measurements of the entire PAni based nanostructured materials were carried out at room temperature using contact angle measurement system from Data Physics instrument GmbH, Germany, model OCA 15 EC [**Figure 3.14**]. To measure the surface energy of the the entire PAni based nanostructured materials, contact angles were measured by using three different liquids including two polar liquids: water and ethylene glycol and one non-polar liquid: diiodomethane.

3.3.8 Fourier transform infrared (FT-IR) spectroscopy

Fourier Transform Infrared Spectroscopy (FT-IR) is a powerful analytical tool for characterization and identification of organic molecules, chemical bonds (functional groups) and the molecular structure of organic compounds. In FT-IR, part of the infrared radiation is absorbed by the sample and the rest is transmitted. The wavelength of infrared radiation absorbed is characteristic of stretching/bending vibrational modes of a chemical bond. The most useful range for identification of the compounds is the near and mid-infrared region as most of the molecular vibrations lie in these frequency regions. The output spectrum demonstrates the molecular

absorption and transmission and thereby, creates a molecular fingerprint of the material being studied with absorption peaks corresponding to the vibration frequencies of the constituent bonds of the atoms. Due to unique combination of atoms in different materials, the infrared spectra of two compounds are never similar. This enables the FT-IR spectroscopy to positively identify the different materials in a qualitative manner. When there is a single change vibrational energy, number of rotational energy changes also take place. Subsequently, bands of the vibrational spectra are observed rather than as discrete lines. These band positions are displayed as wave numbers (in cm^{-1}), while the band intensities are depicted in terms of transmittance 'T', which is the ratio of the radiant power transmitted by the sample or the absorbance 'A', given by, A = log10(1/T). Determination of frequencies, at which the material absorbs IR radiation, allows the identification of the material's chemical constituents, since each functional group absorbs radiation at a certain specific frequency. In addition, the intensity of the peaks in the spectrum indicates the amount of material present. With modern software algorithms, infrared is an excellent tool for quantitative analysis. The FTIR spectroscopy study of the entire synthesized materials have been conducted using a Perkin Elmer spectrum 100 spectrophotometer installed at Tezpur University, Assam, India.

3.3.9 Nuclear magnetic resonance (NMR) spectroscopy

The NMR phenomenon is based on the fact that nuclei of atoms have magnetic properties that can be utilized to yield chemical information. Quantum mechanically subatomic particles (protons, neutrons and electrons) have spin. In some atoms (eg ^{12}C, ^{16}O, ^{32}S) these spins are paired and cancel each other out so that the nucleus of the atom has no overall spin. However, in many atoms (^{1}H,^{13}C, ^{31}P, ^{15}N, ^{19}F etc) the nucleus does possess an overall spin. In the absence of an applied magnetic field, all the spins of a given nucleus are of equivalent energy and in a collection of atoms, all of the spin states should be almost equally populated, with the same number of atoms having each of the allowed spins. However, under the application of an external magnetic field, spin states are not of equivalent energy since being the charged particle, the nucleus when moving generates its own magnetic field and hence possess magnetic moment (μ). For instance, in an applied magnetic field all the protons have their magnetic moments (μ) either aligned with the field or opposed to it. The nuclear magnetic resonance phenomenon occurs when nuclei aligned with an applied field are

induced to absorb energy and change their spin orientation with respect to the applied field.

The ^{1}H NMR spectra of the various PAni nanofiber materials were recorded using 400 MHz NMR spectrophotometer, Jeol model ECS 400 installed at Department of Chemical Science, Tezpur University, India. The characterization was carried out in polar solvent dimethyl sulfoxide (DMSO) due to poor solubility of PAni in other organic solvents. Tetramethylsilane (TMS) was used as a standard reference substance in solution and the resonance frequency of each protons in the sample was measured relative to the resonance frequency of the protons of the reference substance.

3.3.10 X-ray photoelectron spectroscopy (XPS)

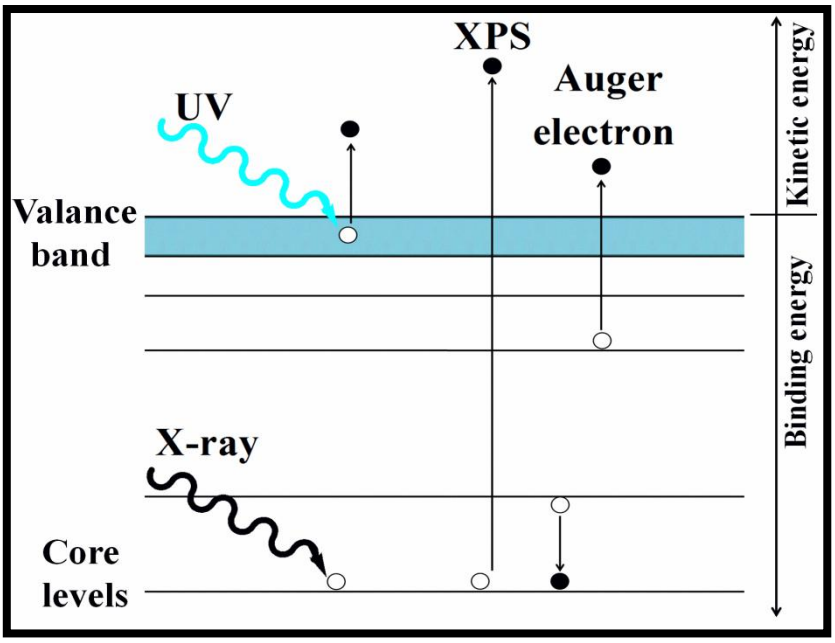

Figure 3.9. An example of a photoelectron emitted due an incident photon.

Photoelectron spectroscopy is a general term that refers to all those techniques based on the application of the photoelectric effect originally observed by Hertz and later explained as a manifestation of the quantum nature of light by Einstein. X-ray photelectron spectroscopy (XPS) is a photoemission experiment for spectroscopic purposes. Photons from soft x-ray radiation are directed on a sample under ultra high vacuum and the photoelectrons emitted from the sample by the photoelectric effect, are analysed with respect to kinetic energy by an electrostatic analyser. With this

technique it is possible to analyse the chemical composition of material surfaces up to 10 nm depth. When photons with the wavelength in the lower energy¸ Xray region are incident on the crystal surface then core electrons are knocked out of atoms **[Figure 3.9]**. Spectrum is obtained by measuring the characteristics of electrons that escape from the surface. According to Einstein, when light is incident on a sample, an electron can absorb a photon and escape from the material with a maximum kinetic energy as follows:

$$E_k = h\upsilon - E_B - \phi \qquad 3.12$$

where υ is the photon frequency, E_B is the electron binding energy and Φ is the work function, which gives the minimum energy required to remove a delocalised electron from the surface of the metal. The work function is a measure of the potential barrier at the surface that prevents the valence electrons from escaping.

XPS was performed using an ESCALAB 250 Xi system (Thermo Scientific) equipped with a monochromated Al Kα X-ray source. Uniform charge neutralization was provided by beams of low-energy (≤10 eV) Ar+ ions and low-energy electrons guided by the magnetic lens. The standard analysis spot of ca. 900×600 μm^2 was defined by the microfocused X-ray source. Full survey scans (step size 1 eV, pass energy 150 eV, dwell time 50mS and 3 scans) and narrow scans (step size 0.1 eV, pass energy 20 eV, dwell time 100 mS and 5 scans) of the C1s (BE ~285 eV) regions were acquired from three separate areas on each sample. Data were transmission function corrected and analyzed using Thermo Avantage Software (Version 5.952) using a smart background.

3.3.11 Ultra violet-visible (UV-Vis) spectroscopy

Ultra violet-visible (UV-Vis) spectroscopy is a type of absorption spectroscopy in the ultraviolet and visible spectral region. In this region of electromagnetic spectrum, molecules typically undergo electronic transitions. Therefore, UV-vis absorption spectroscopy technique provides key information about the electronic transitions and the electronic structure of the material. Ultraviolet and visible radiation interacts with matter which causes electronic transitions from ground state to high energy states. Different types of electronic transitions are possible in a molecule which includes: σ-σ^* (alkanes), σ-π^* (carbonyl compounds), π-π^* (alkenes, carbonyl compounds, alkynes, azo compounds), n-σ^* (oxygen, nitrogen, sulphur and halogen compounds)

and n-π^* (carbonyl compounds). Transition from the highest occupied molecular orbital (HOMO) to the lowest unoccupied molecular orbital (LUMO) requires the least amount of energy and is the most favourable transition. On the other hand, some of the electronic transitions are "forbidden" by certain selection rules. UV-Vis spectroscopy study of different PAni nanofibers was conducted using a Shimadzu model UV-2450 spectrophotometer. Absorbance in the range of 200-900 nm was recorded using quartz cuvettes of 1 cm of path length by dispersing samples in phosphate buffer saline (PBS, pH=7.4).

3.3.12 Fluorescence spectroscopy

Fluorescence spectrometry is a fast, simple and inexpensive method to determine the concentration of an analyte in solution based on its fluorescent properties. It can be used for relatively simple analyses, where the type of compound to be analyzed is known, to do a quantitative analysis to determine the concentration of the analyte. In fluorescence spectroscopy, a beam with a wavelength varying between 180 and ~800 nm passes through a solution in a cuvette and the light that is emitted by the sample is mesaured. In fluorescence spectrometry both an excitation spectrum (the light that is absorbed by the sample) and/or an emission spectrum (the light emitted by the sample) can be measured. The concentration of the analyte is directly proportional with the intensity of the emission.

UV-Vis spectroscopy study of different PAni nanofibers was conducted using a photoluminescence spectrometer (LS 55, PERKIN ELMER). Emission in the range of 300-700 nm was recorded using quartz cuvettes of 1 cm of path length by dispersing samples in phosphate buffer saline (PBS, pH=7.4) at an excitation wavelength 250-280 nm.

3.3.13 Stability test

To investigate the degradation and stability, the as-synthesized materials were incubated in a physiological solution of phosphate buffer saline (PBS, pH=7.4) at 37°C. The non-functionalized and the functionalized films of PAni nanofibers were incubated for 30 days. The non-functionalized and the functionalized films of PAni:Ch nanocomposites were incubated for 15 days, while different electrospun MEH-PPV:PCL nanofibers were incubated for 45 days. Degradation and stability of

the materials were evaluated by SEM and measurements of current-voltage (*I-V*) characteristics after of incubation in PBS. Percentage of weight loss after incubation in PBS has been measured using the following formula:

$$\%\, Weight\ loss = \frac{Change\ in\ weight\ after\ incubation\ in\ PBS\ (in\ mg)}{Original\ weight\ before\ incubation\ in\ PBS\ (in\ mg)} \times 100\% \quad 3.13$$

For SEM images, the samples were washed with deionized water twice to remove salts and air dried. Measurements for *I-V* characteristics were performed three times for each sample and sheet resistance (R_s) values were determined as discussed above to check the conductive properties in physiological condition.

3.4 Biochemical properties

3.4.1 Urease immobilization

Immobilization of urease on PAni:Ch nanocomposite films was performed by immersing the films into urease solution. In a typical procedure, urease solution was prepared by dissolving urease (activity 370 unit/mg) in phosphate buffer solution (pH = 7.4) with a concentration of 1mg/mL. The non-functionalized and functionalized PAn:Ch nanocomposite films with 4 wt% and 6 wt% of PAni content of dimension 1.5 cm × 1.5 cm were used for the immobilization purpose. Thereafter, the films were immersed in urease solution for 24 h at 4°C. After immobilization, the films were washed thrice with milli Q water.

3.4.2 Urease activity test

The activity of both, immobilized and free, urease was determined using Nessler's method by measuring the amount of ammonia liberated in the urease-catalyzed reaction of hydrolysis of urea per unit time spectrophotometrically [318]. To conduct the activity test, the washed films were treated with 200 µl of urea solution with different concentrations viz., 20, 40, 60, 80 and 100 mM. Urease catalyzes the hydrolysis of urea into carbon dioxide and ammonia as follows:

$$(NH_2)_2CO + H_2O \rightarrow CO_2 + 2NH_3$$

Subsequently, 100 µl of Nessler's reagent was added to the reaction solution, which results the yellowish appearance upon hydrolysis of urea. The produced ammonia

reacts with Nessler's reagent to form a yellow colored product giving maximum absorbance at 470 nm:

$$2K_2HgI_4 + NH_3 + KOH \rightarrow HgO.Hg(NH_3)I \downarrow + 2H_2O$$

Nessler's reagent Yellow color

The intensity of the absorbance is proportional to the active immobilized urease on the nanocomposite films [189]. Briefly, the activity of free urease and immobilized urease was determined using the following formula:

$$Urease\ activity\left(\frac{\mu mol.min^{-1}}{mg}\right) = \frac{OD_{sample} - OD_{PBS}}{Slope \times t \times Protein\ content\ in\ mg} \times n \quad 3.14$$

Here, OD_{sample} and OD_{PBS} are the measured absorbance values of sample and enzyme buffer, respectively, t is the incubation time and n is the dilution factor. The protein content is determined by measuring the difference in weight of the substrate (Dimension: 1.5 cm× 1.5 cm) before and after immobilization of urease (Concentration: 1 mg/mL). In the present thesis, the activity of urease immobilized on different PAni:Ch nanocomposites was measured at 10 min interval throughout an hour and at different pH = 2, 4, 6, 8 & 10. All the experiments were repeated for n=3. All the urease activity assays were performed in collaboration with "Cancer Genetics and Chemoprevention Research Group" of Prof. Anand Ramteke, Department of Molecular Biology and Biotechnology, Tezpur University, Tezpur.

3.5 Biological characterization

3.5.1 Hemolysis activity assay

Materials intended for biomedical applications require their characterization by hemocompatibility, also known as blood compatibility. The hemolysis activity assay for all the samples has been carried out with the help of research scholars of "Cancer Genetics and Chemoprevention Research Group" of Prof. Anand Ramteke, Department of Department of Molecular Biology and Biotechnology, Tezpur University, Tezpur. The collection of blood from healthy volunteers (who were not under medication) was approved by the Tezpur University Ethical Committee and informed consent was obtained from all participants. Hemocompatibility of a material depends on material-blood interaction and controlled by the properties of both the material and the blood. Direct evidence of damages due to the action of test material on erythrocyte membranes can be obtained by measuring the extent of hemolysis, i.e.

the leakage of hemoglobin from the cytoplasm. The hemolytic activity of all the materials reported in the present study was performed as described elsewhere with slight modification [319]. Fresh human blood was collected from healthy donors among laboratory personnel. Citrate buffer was used as anticoagulant. Erythrocytes were separated from plasma and buffy coat by centrifugation at 800×g, 10 min, and washed three times in isotonic phosphate buffer saline (PBS, pH=7.4). After three washings with the phosphate-buffered saline solution (centrifugation for 5 min at 700 g), the erythrocytes were suspended in 20 mL PBS. A 5% (v/v) suspension of erythrocytes in PBS was prepared and treated with 2 mg of each sample. After 35 min incubation at 37^0 C, agitate the cells for 10min on ice followed by centrifugation at 1300g for 5 min. After that, supernatant was taken and absorbance was read at 540 nm against reagent blank and the percentage membrane activity was calculated by comparing the test with positive (Triton-x100) and negative (PBS) control. Hemolysis is destruction of red blood cells (RBCs) either by chemical or mechanical stress to an erythrocyte that causes the release of hemoglobin in the surrounding media and can be readily quantified using spectrophotometry. Hemolysis activity is measured by measuring the optical density at 540 nm using an ultraviolet spectrophotometer and the percentage of hemolysis is calculated using the following formula:

$$\%\, Haemolysis = \frac{OD_{Sample} - OD_{negative\ control}}{OD_{positive\ control} - OD_{negative\ control}} \times 100 \qquad 3.15$$

Here, Triton X-100 has been used as positive control, which induces 100% hemolysis and phosphate buffer saline (PBS, pH=7.4) has been used as negative control, which causes no damage to RBCs.

3.5.2 Cell culture

The CP based biomaterials synthesized in the present study were investigated with three cell lines to evaluate the potential of these materials in various tissue engineering applications. The non-functionalized and functionalized PAni nanofibers were studied with breast cancer MDA-MB-231 cell line. The non-functionalized and glutaraldehyde functionalized PAni:Ch nanocomposites were investigated with MDA-MB-231 cell line, while the glycine NHS ester functionalized PAni:Ch nanocomposites were tested as a biomaterial scaffold with 3T3 fibroblasts. Similarly, to evaluate the potential of collagen coated PAni:Ch nanocomposites and different

electrospun MEH-PPV:PCL nanofibers in neural tissue engineering, a rat neuronal model pheochromocytoma PC12 cell line was used. The non-functionalized and functionalized electrospun MEH-PPV:PCL nanofibers were also studied with 3T3 fibroblasts. The culture protocols of these cell lines are discussed below.

3.5.2.1 MDA-MB-231 cell culture

A breast cancer MDA-MB-231 cell line (P5) (ATCC® HTB-26™) was cultured in Leibovitz's L-15 medium (Sigma) supplemented with 10% fetal bovine serum (FBS, Sigma) and 1 % penicillin-streptomycin (Pen Strep, Sigma) were incubated at 37°C in 5% CO_2. Cells were passaged at 80-85% confluence using a 0.25% trypsin-ethylenediaminetetraacetic acid (trypsin-EDTA) solution (Sigma). During experimentation, cells were directly cultured on the materials.

3.5.2.2 3T3 cell culture

A mouse embryonic 3T3 fibroblast cell line (P15), NIH 3T3 (ATCC® CRL-1658TM) was used to investigate the impact of different CP based materials on cell viability including other cellular activities such as cell adhesion, spreading and proliferation. Cells were cultured in Dulbecco's modified Eagle's medium (DMEM) supplemented with 10% FBS and 1% penicillin-streptomycin (Pen Strep) and were incubated at 37°C in 5% CO_2. Cells were passaged weekly using a 0.25% trypsin–EDTA solution (Sigma). During experimentation, cells were directly cultured on the materials.

3.5.2.3 PC12 cell culture

A PC-12 (ATCC® CRL-1721™) cell line (P3) was cultured in RPMI-1640 media (Sigma-Aldrich) supplemented with 10% horse serum (Hyclone), 5% FBS (Hyclone) and 1% penicillin-streptomycin solution (Sigma-Aldrich) and were incubated at 37°C in 5% CO_2. Cells were passaged weekly using a 0.25% trypsin–EDTA solution (Sigma). For differentiation study, the growth medium was changed to differentiating medium containing RPMI-1640 supplemented with 1% horse serum, 1% penicillin-streptomycin solution and 100 ng/mL nerve growth factor (NGF, Sigma-Aldrich) for neuronal differentiation after 24 h of culture. During experimentation, cells were directly cultured on the materials.

3.5.3 Sample preparation for cell culture

All the samples (film or mesh) were cut using biopsy punch in a circular shape with diameters of 5 mm for cytotoxicity test and 10 mm for live/dead assay, immunostaining, and cell morphology study. Since PC12 cells adhere poorly to tissue culture plastic, 96 well tissue culture plate was coated with 0.01% Collagen I from rat tail (Sigma) in 0.1 M acetic acid for cytotoxicity test. One set of PAni:Ch nanocomposites films and all the electrospun meshes were also similarly coated with 0.01% Collagen I in 0.1 M acetic acid. Before all cell culture experiments, all the samples were kept in sterile PBS for 24 h and sterilized under UV light for 1h each side of the films. For electrical stimulation experiment, electrospun meshes of diameter 15 mm were used.

3.5.4 MTS proliferation assay

The MTS proliferation assay was carried out to evaluate the cytotoxicity of the materials reported herein. The PAni nanofibers and PAni:Ch nanocomposites before and after surface functionalization by glutaraldehyde were tested for cell viability with MDA-MB-231 cells in collaboration with "Cancer Genetics and Chemoprevention Research Group" of Prof. Anand Ramteke, Department of Molecular Biology and Biotechnology, Tezpur University, Tezpur. Cell viability on the glycine NHS ester functionalized PAni:Ch nanocomposites was studied with 3T3 fibroblasts and PC12 cells in Biomaterials and Medical Devices Research Laboratory, University of Brighton, United Kingdom. Similarly, cytotoxicity of all the non-functionalized and functionalized electrospun MEH-PPV:PCL nanofibers was evaluated with 3T3 fibroblasts and PC12 cells using MTS proliferation assay.

Metabolically active cells are capable of reducing a tetrazolium compound into a water soluble formazan product. Non-viable cells rapidly lose their ability to reduce 3-(4,5-dimethylthiazol-2-yl)-5-(3- carboxymethoxyphenyl)-2-(4-sulfophenyl)-2H-tetrazolium, inner salt) (MTS). Therefore, the production of the coloured formazan product is proportional to the number of viable cells [320]. MDA-MB-231 and 3T3 cells were seeded on different substrates at a concentration of 5×10^3 cells/well in a 96 well plate for the MTS assay. PC12 cells were cultured in growth medium at a concentration of 1×10^4 cells/well in direct contact. Cell viability after 24 h incubation on the materials was quantified using Promega™ CellTiter 96™

AQueous One Solution Cell Proliferation Assay (MTS) (Fisher Scientific). The cultured materials were washed with sterile PBS twice, and MTS reagent diluted 1:5 in media was added directly to all the wells except the blank. Plates were incubated for 2 h at 37°C and optical density (OD) was measured at 490 nm.

The percentage of cell viability has been calculated using the following formula:

$$\%\ Cell\ viability = \frac{OD_{sample} - OD_{blank}}{OD_{-ve\ control} - OD_{blank}} \times 100\% \qquad 3.16$$

Here, OD_{sample} is the optical density of the cells cultured on sample in cell media, $OD_{-ve\ control}$ is the optical density of the cells cultured on tissue culture plastic only (negative control) and OD_{blank} is the optical density of cell media only (without cells). The negative control is believed to induce maximum cell viability, whereas the positive control (*tert* butyl maleate) causes maximum cell death. All the experiments were performed at n = 6.

3.5.5 Acridine orange/ethidium bromide (AO/EtBr) staining

Acridine orange/ethidium bromide (AO/EB) dual staining was used to visualize nuclear changes and apoptotic body formation that are characteristic of apoptosis [321]. The AO/EtBr staining of MDA-MB-231 cells has been performed in "Cancer Genetics and Chemoprevention Research Laboratory" of Prof. Anand Ramteke, Department of Molecular Biology and Biotechnology, Tezpur University, Tezpur. AO is a cell-permeable dye taken up by both viable and nonviable cells to emit green fluorescence if intercalated into double stranded nucleic acid (DNA) or red fluorescence if bound to single stranded nucleic acid (RNA). EtBr, a membrane-impermeable dye is taken up only by cells with a compromised cell membrane and emits red fluorescence on intercalation into DNA. Four types of cell population can be studied according to the fluorescence emission and the morphological aspect of chromatin condensation in the stained nuclei: (i) Viable cells have uniform bright green nuclei with an organized structure (ii) Early apoptotic cells (which still have intact membranes but have started to undergo DNA cleavage) have green nuclei, but perinuclear chromatin condensation is visible as bright green patches or fragments (iii) Late apoptotic cells have orange to red nuclei with condensed or fragmented

chromatin and (iv) Necrotic cells have uniformly orange to red nuclei with a condensed structure.

Briefly, 50 mg of EtBr and 15 mg of AO were dissolved in 1ml of 95% ethanol and 49 ml of distilled water, which was divided into 50 aliquots containing 1 ml each, treated as stock solution. This stock solution was diluted to 100 times in PBS prior to experimentation. MDA-MB-231 cells were cultured on the PAni films and PAni:Ch nanocomposites films of cut into circular shape of diameter of 10 mm in a 48 well plate tissue culture plate following the procedure as discussed **in Subsection 3.5.2.1**. The concentration of cell was 5×10^3 cells/well. Staining was performed after 3 days of culture. MDA-MB-231 cells cultured on the PAni films and PAni:Ch nanocomposites films were washed with sterile PBS thrice and transferred to a new 48 well plate. Then, 10 □L of AO/EtBr was added to each well and incubated for 5 min at room temperature. After incubation, films with the cells were again washed with PBS thrice and viewed directly under Fluorescence microscope (LEICA DM 3000, power = ebq 50 qc, USA) attached to a LEICA DFC 450C camera. The experiment was conducted for n=4.

3.5.6 Live/dead assay

Live/dead assay was used to visualize difference in cell viability on the non-functionalized and surface functionalized PAni:Ch nanocomposites films and electrospun MEH-PPV:PCL nanofibers. Live/dead staining of 3T3 cells using ethidium homodimer-1 (EthD-1, Thermo Fisher Scientific) (staining dead cells in red), calcein AM (Thermo Fisher Scientific) (staining live cells in green) and 4',6-Diamidino-2-Phenylindole, Dihydrochloride (DAPI, Thermo Fisher Scientific) (staining nucleic acid in blue), were carried out in Biomaterials and Medical Devices Research Laboratory, University of Brighton, United Kingdom [324, 323]. Cells were seeded at a concentration of 1×10^4 cells/well in a 48 well plate for the live/dead assay for time points of 24 h and 48 h. The live/dead assay was used to monitor the morphology and spreading of 3T3 fibroblasts at three different time points namely 24 h and 48 h so that cell behaviour on non-functionalized and surface functionalized surfaces can be distinguished. The scaffolds seeded with 3T3 fibroblasts were washed with sterile PBS thrice prior to staining and transferred to a new culture plate. Cells were stained with a solution of 4 μM EthD-1, 2 μM calcein AM and 20 μL of DAPI in PBS and were then incubated for 30 min at room temperature before evaluation.

The experiments with each substrate was carried out for n=6. The stained cells were imaged using Leica TCS SP5 Confocal Laser Scanning Microscope [CLSM] (Leica Microsystems, UK).

3.5.7 Beta (III) tubulin immunochemistry

Immunocytochemistry was performed using neuronal marker beta III-tubulin to confirm the differentiation of the PC12 cells in Biomaterials and Medical Devices Research Laboratory, University of Brighton, United Kingdom [324, 325]. PC12 cells were cultured on the functionalized and collagen I coated PAni:Ch nanocomposites films and electrospun meshes in differentiating medium at a concentration of 1×10^5 cells/well for 7 days. Cells were washed in PBS, fixed in 100% methanol for 5 min, washed thrice in PBS then incubated with blocking and permeabilizing solution of 1% bovine serum albumin (BSA, Sigma-Aldrich), 10% (v/v) normal goat serum (Sigma-Aldrich) and 0.3 M glycine (Acros Organics) in 0.1% (v/v) tween PBS for 1 h. The cells were incubated with primary antibody Rb pAb to anti beta III tubulin (ab18207, Abcam, UK), at a concentration of 5 μg/mL overnight at 40°C, washed thrice in PBS then incubated with secondary antibody Goat pAb to Rb IgG Alexa fluor 488 (ab150077, Abcam, UK) at a concentration of 2 μg/mL for 1h at room temperature. The cells were stained with DAPI for nuclei counterstaining and imaged using confocal microscopy. The experiment was conducted for n=6. The stained cells were imaged using Leica TCS SP5 Confocal Laser Scanning Microscope [CLSM] (Leica Microsystems, UK).

3.5.8 Image analysis

Fluorescent images of MDA-MB-231 cells and 3T3 fibroblasts cultured on different substrates acquired after AO/EB staining and live/dead assay, respectively, were processed in ImageJ software for determination of viable cell density. Cell area and spreading were also analyzed in ImageJ software using the fluorescent images. Morphological analysis was limited to the cells, which were not in physical contact with more than one cell [323]. The cells that adopted elongated, polygonal shape, with filopodia- or lamellipodia-like extensions were regarded as spreading cells [323]. In contrast, the cells that retained round morphology were regarded as non spreading cells. Cell spreading was evaluated in terms of percent of spreading by dividing the number of spread cells by the total number of cells that bound to the substartes. To

ensure a representative count or measurement, each sample was divided into quarters and two fields per each quarter were photographed in an area of approximately 0.15 mm^2.

The number of PC12 cells on various substrates was determined by counting nuclei stained with DAPI dye from confocal images. The total number of cells were counted in 3 fields of view (top, centre and down) for each of three repeat samples per substrate type. Neurite length was measured as a linear distance between the cell junction and the tip of a neurite. For PC12 cells, data was collected for neurite lengths at least as long as twice the diameter of the cell body [324]. Neurite outgrowth was reported in terms of neurite length per cell (for cells that expressed at least one neurite) and median neurite length. Also, the percentages of PC12 cells with neurites and the numbers of neurites per cell (for cells that expressed at least one neurite) were calculated. In the case of neurites with an ambiguous origin, the longest neurite was retained for the measurements to prevent repeated sampling of the same neurite segment within each image.

3.5.9 Cell adhesion test

3.5.9.1 MDA-MB-231 cell attachment

SEM was performed to study the morphology and adhesion of MDA-MB-231 cells on different PAni nanofibers films and PAni:Ch nanocomposites films after 3 days. The 3T3 cells were rinsed with phosphate buffer saline (PBS) and fixed with 4% glutaraldehyde solution at 40°C for 30 min.

3.5.9.2 3T3 cell attachment

SEM was performed to study the morphology and adhesion of 3T3 cells cultured on non-functionalized and functionalized samples after 3 days. The 3T3 cells were rinsed with phosphate buffer saline (PBS) and fixed with 4% glutaraldehyde solution at 40°C for 30 min.

3.5.9.3 PC12 cell attachment

Cell proliferation and differentiated PC12 morphology on uncoated, surface functionalized and collagen coated substrates were evaluated using SEM after 7 days of culture. All CP based substrates seeded with PC12 cells were rinsed with phosphate

buffer saline (PBS) and fixed with 4% glutaraldehyde solution for 45 min at 4°C. Cell seeded scaffolds were then dehydrated by incubation with serially increasing concentrations of ethanol beginning with incubation in 30% ethanol for 1 h then, 50%, 60%, 70%, 80%, 90% and absolute ethanol for 10 min each. The dehydrated cell seeded scaffolds were air dried overnight prior to SEM analysis.

3.6 Electrical stimulation of PC12 cells

Electrical stimulation of PC12 cells was performed on different CP based scaffolds reported in the present study according to the experimental condition as previously reported but with a slight modification [155, 326, 327]. The electrical stimulation experiment was set up as shown in the schematic in **Figure 3.10 (a)**. Briefly, an Ag wire was connected to a 15 mm diameter CP based scaffold and was used as the working electrode (WE). The CP based scaffold connected to the Ag wires were fixed in a 24 well tissue culture plate. Thincert cell culture inserts (24 Well ThinCert™ Cell Culture Inserts, Greiner, New Zealand) with an inner diameter of 8.4 mm, height of 16.25 mm and working volume 0.4 mL - 1.2 mL, were fixed onto the electrospun meshes in a 24 well plate after removing the bottom membrane. The edges of the insert were sealed using poly(dimethylsiloxane) (PDMS, SYLGARD®184, Sigma) to prevent any direct contact between the cell culture medium and the Ag wire connected to the CP based scaffold. A Pt wire placed in the cell culture medium, at a distance of 1 cm from the WE, was used as counter electrode (CE) [**Figure 3.10 (a)**]. The CP based scaffolds were washed thrice with sterile deionized water and incubated in sterile PBS solution overnight. The whole assembly was sterilized under UV for 3 h. PC12 cells were cultured at 1×10^3 cells/well in growth medium, and after 24 h of culture, growth medium was replaced with differentiating medium containing NGF. Then, a constant electrical potential of 500 mV/cm was applied across the electrodes for 2 h/day for 3 consecutive days using a portable bipotentiostat (EmStat Blue, PalmSens BV, Netherlands).

The electrical stimulation was carried out by a double pulsed potential chronoamperometric technique in an incubator [**Figure 3.10 (c)**]. The electrically stimulated PC12 cells were cultured for another 72 h without electrical stimulation. For comparison, PC12 cells on all the CP based scaffold without electrical stimulation were also cultured under the same condition for 7 days treated as control. The

differentiating medium was changed every 2 days during the experimental period. All the experiments were performed in triplicate.

The electrical stimulation was also performed under a constant electrical potential of 100 and 200 mV/cm, however, the current signals through the scaffolds were observed to be very low and we did not find any improvement in PC12 differentiation or neurite outgrowth. Therefore, those results have not been presented in the thesis. The same cell culture plates where the electrical stimulation experiment was performed have been used for immunostaining purpose after removing the wire contacts. The rest of the immunostaining procedures are similar as described in **Section 3.5.7**. The electrical stimulation experiment was carried out in Biomaterials and Medical Devices Research Laboratory, University of Brighton, United Kingdom.

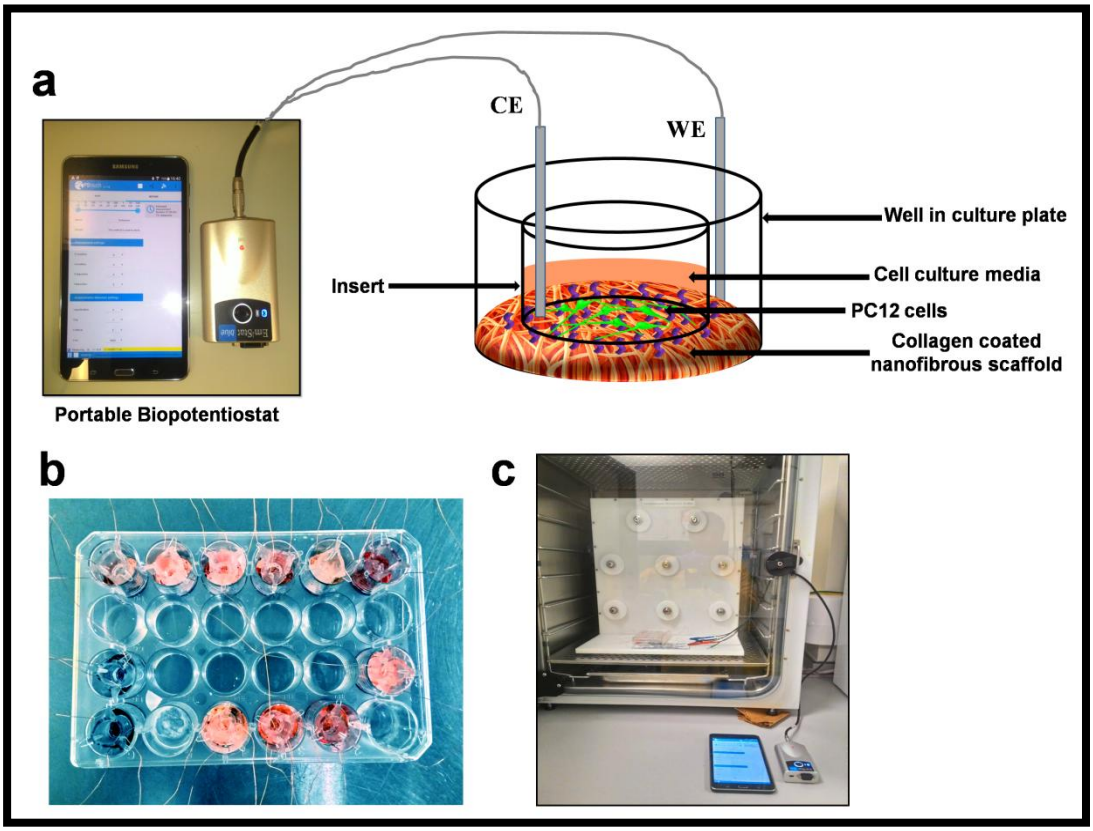

Figure 3.10. (a) Schematic illustration of the electrical stimulation experiment using a custom made electrical stimulation set up ; (b) photograph of self made cell culture plate with different CP based scaffolds fixed on it for electrical stimulation experiment; (c) photograph of the electrical stimulation experiment *in situ*.

3.7 Statistical analysis

All experiments for statistical analysis were repeated with a minimum of n = 3. Statistical analysis was performed using one-way analysis of variance (ANOVA) with Fisher's Least Significant Difference (LSD) post hoc test in MS excel [328]. The Least Significant Difference (LSD) between any two groups a and b with a number of observations N_a and N_b, respectively, provided the ANOVA F omnibus is significant, was calculated by using the following formula:

$$LSD = t_{v,\alpha}\sqrt{MSW\left(\frac{1}{N_a}-\frac{1}{N_b}\right)} \qquad 3.15$$

Where *MSW* denotes the mean square of error within group and $t_{\upsilon,\alpha}$ is the value of t statistics at level of significance α with degrees of freedom ν. Statistically significant values were defined at α=0.05 or 0.01, whichever is applicable.